THE JOURNAL OF BIOLOGICAL CHEMISTRY VOL. 289, NO. 4, pp. 2127–2138, January 24, 2014

Residues in the Polar Loop of Subunit *c* in *Escherichia coli* ATP Synthase Function in Gating Proton Transport to the Cytoplasm*

Received for publication, October 25, 2013, and in revised form, December 1, 2013 Published, JBC Papers in Press, December 2, 2013, DOI 10.1074/jbc.M113.527879

P. Ryan Steed and Robert H. Fillingame[1]

From the Department of Biomolecular Chemistry, School of Medicine and Public Health, University of Wisconsin, Madison, Wisconsin 53706

Background: H^+ transport through membrane-traversing ATP synthase mechanically drives bond formation.
Results: Metal chelation with cysteine residues in cytoplasmic domains near the surface of the membrane blocks proton transport.
Conclusion: Gating from the H^+ channel traversing the lipid bilayer occurs in cytoplasmic loops of transmembrane proteins.
Significance: The proton transport pathway traversing ATP synthase extends beyond the lipid bilayer into the cytoplasm.

Rotary catalysis in F_1F_0 ATP synthase is powered by proton translocation through the membrane-embedded F_0 sector. Proton binding and release occur in the middle of the membrane at Asp-61 on the second transmembrane helix (TMH) of subunit *c*, which folds in a hairpin-like structure with two TMHs. Previously, the aqueous accessibility of Cys substitutions in the transmembrane regions of subunit *c* was probed by testing the inhibitory effects of Ag^+ or Cd^{2+} on function, which revealed extensive aqueous access in the region around Asp-61 and on the half of TMH2 extending to the cytoplasm. In the current study, we surveyed the Ag^+ and Cd^{2+} sensitivity of Cys substitutions in the loop of the helical hairpin and used a variety of assays to categorize the mechanisms by which Ag^+ or Cd^{2+} chelation with the Cys thiolates caused inhibition. We identified two distinct metal-sensitive regions in the cytoplasmic loop where function was inhibited by different mechanisms. Metal binding to Cys substitutions in the N-terminal half of the loop resulted in an uncoupling of F_1 from F_0 with release of F_1 from the membrane. In contrast, substitutions in the C-terminal half of the loop retained membrane-bound F_1 after metal treatment. In several of these cases, inhibition was shown to be due to blockage of passive H^+ translocation through F_0 as assayed with F_0 reconstituted into liposomes. The results suggest that the C-terminal domain of the cytoplasmic loop may function in gating H^+ translocation to the cytoplasm.

F_1F_0 ATP synthase utilizes the energy stored in an H^+ or Na^+ electrochemical gradient to synthesize ATP in bacteria, mitochondria, and chloroplasts (1–3). The ATP synthase complex is composed of two sectors, *i.e.* a water-soluble F_1 sector that is bound to a membrane-embedded F_0 sector. In eubacteria, F_1 is composed of five subunits in an $\alpha_3\beta_3\gamma\delta\epsilon$ ratio and contains three catalytic sites for ATP synthesis and/or hydrolysis centered at the α-β subunit interfaces. F_0 is composed of three subunits in an $a_1b_2c_{10-15}$ ratio in eubacteria and functions as the ion-conducting pathway (4–8). The *c*-ring composition in mitochondria varies between species, being eight for bovine and 10 in yeast (9, 10). Ion translocation through F_0 drives rotation of a cylindrical ring of *c* subunits that is coupled to rotation of the γ subunit within the $(\alpha\beta)_3$ hexamer of F_1 to force conformational changes in the three active sites and in turn drive synthesis of ATP by the binding change mechanism (1–3, 11–14).

Subunit *c* of F_0 folds in the membrane as a hairpin of two extended α-helices connected by a short cytoplasmic loop. In *Escherichia coli*, 10 copies of subunit *c* pack together to form a decameric cylindrical ring with TMH1[2] on the inside and TMH2 on the periphery (5, 15, 16). In the atomic resolution structures of H^+-translocating c_{14}-ring from spinach chloroplast (17, 18) and the c_{15}-ring from *Spirulina platensis* (19), the H^+-binding Glu, which corresponds to Asp-61 in *E. coli*, is located in TMH2 at the middle of the lipid bilayer. Several other neighboring residues form a hydrogen bonding network between TMHs 1 and 2 of one subunit and TMH2 from the adjacent subunit. A more recent structure of the c_{13}-ring from *Bacillus pseudofirmus* OF4 (20) revealed a more hydrophobic H^+ binding site in which a water molecule is coordinated by the H^+-binding Glu and the backbone of the adjacent TMH2, an architecture likely shared by the *E. coli c*-ring. The loop of subunit *c*, particularly a conserved R(Q/N)P motif, is involved in binding the γ and ϵ subunits of F_1 and coupling H^+ translocation to ATP synthesis/hydrolysis (21–30).

Subunit *a* consists of five transmembrane helices, four of which likely interact as a four-helix bundle (31–34). Subunit *a* lies on the periphery of the *c*-ring with TMHs 4 and 5 from subunit *a* and TMH2 from subunit *c* forming the *a*-*c* interface (35, 36). During ion translocation through F_0, the essential Arg-210 on TMH4 of subunit *a* is postulated to facilitate the proto-

* This work was supported, in whole or in part, by National Institutes of Health Grant GM23105 from the United States Public Health Service.
[1] To whom correspondence should be addressed: Dept. of Biomolecular Chemistry, University of Wisconsin, 420 Henry Mall, Madison, WI 53706. Tel.: 608-262-1439; Fax: 608-262-5253; E-mail: rhfillin@wisc.edu.

[2] The abbreviations used are: TMH, transmembrane helix; ACMA, 9-amino-6-chloro-2-methoxyacridine; β-MSH, β-mercaptoethanol; DCCD, dicyclohexylcarbodiimide; Tricine, *N*-[2-hydroxy-1,1-bis(hydroxymethyl)-ethyl]glycine.

nation/deprotonation cycle at Asp-61 of subunit *c* and cause the rotation of the *c*-ring past the stationary subunit *a* (2, 3, 37).

Chemical modification of cysteine-substituted transmembrane proteins has been widely used as a means of probing the aqueous accessible regions (38–40). The reactivity of a substituted cysteine to thiolate-directed probes provides an indication of aqueous accessibility because the reactive thiolate species is preferentially formed in an aqueous environment. The aqueous accessibility of subunits *a* and *c* in *E. coli* F_0 has been probed using Ag^+, Cd^{2+}, and other thiolate-reactive probes (37, 41–47). The results suggested the presence of an aqueous accessible channel in subunit *a* in the center of TMHs 2–5 extending from the periplasm to the center of the membrane (34, 36, 37, 44). Protons entering through this periplasmic access channel are postulated to bind to the essential Asp-61 residues of the *c*-ring with the protonation and deprotonation of Asp-61 driving *c*-ring rotation. A second putative channel was suggested at the interface of TMH4 of subunit *a* and TMH2 of subunit *c*, providing an exit pathway at the *a*-*c* interface leading from Asp-61 to the cytoplasm (47).

In previous studies (46, 47), we probed the thiolate reactivity of Cys substitutions in the transmembrane regions of subunit *c* based upon inhibition of function in response to Ag^+ or Cd^{2+} treatment. Here we report on the reactivity of Cys substitutions in the cytoplasmic loop and at the N- and C-terminal ends of subunit *c*, completing the screening of nearly all residues in the subunit. The sensitivity of function to inhibition by Ag^+ and Cd^{2+} proved to be widespread in the loop. Inhibition in this region was surprising because metal chelation to the transmembrane Cys thiolates was thought to inhibit function by blocking proton translocation through F_0, a function in which the loop was not thought to directly participate. We sought to distinguish between several possible mechanisms of inhibition by Ag^+ and Cd^{2+}. Our experiments support the well characterized role of the loop in F_1 binding, which proved to be disrupted by Ag^+ and Cd^{2+} in some substitutions, but also suggest involvement of a distinct section of the loop in gating H^+ transport to the cytoplasm. In light of this and other data, we hypothesize that the aqueous half-channel from the middle of the membrane to the cytoplasm continues through a cytoplasmic domain at the subunit *a*-*c* interface formed by cytoplasmic loops from both subunits.

EXPERIMENTAL PROCEDURES

Strain Construction—The mutagenesis procedure of Barik (48) described previously (46, 47) was used to generate the Cys substitutions in subunit *c*, and all substitutions were expressed in plasmid pCMA113 (41). Fused subunit *c* dimers containing a single Cys substitution in the C-terminal copy were generated from plasmid pPJC2R, which encodes two *c* subunits joined by a short linker (49). For purification of wild type and mutant F_1F_0 complexes, mutant *uncE* was excised from the pCMA113 derivative plasmid and transferred into pFV2 between the PflMI and BssHII restriction sites (50). Like pCMA113, pFV2 codes a Cysless F_1F_0 complex; however, a His tag is present at the N terminus of subunit β rather than subunit *a* (50). The presence of modifications in either plasmid was confirmed by DNA sequencing through the ligation sites. Mutant plasmids were transferred into the chromosomal *unc* (*atp*) operon deletion strain JWP292 (5) for growth and biochemical characterization or DK8 (51) for purification. Growth yields of the mutant strains on glucose minimal medium and succinate minimal medium agar plates were assayed as described previously (41).

ATP-driven ACMA Fluorescence Quenching—Inside-out membrane vesicles were prepared from JWP292 transformant strains, and protein concentrations were determined as described previously (46). Aliquots of membranes (1.6 mg at 10 mg/ml) were suspended in 3.2 ml of HMK-NO_3 buffer (10 mM HEPES-KOH, 1 mM $Mg(NO_3)_2$, 10 mM KNO_3, pH 7.5) or HMK-Cl buffer (10 mM HEPES-KOH, 5 mM $MgCl_2$, 300 mM KCl, pH 7.5) and incubated at room temperature for 10 min. ACMA was added to 0.3 μg/ml, and fluorescence quenching was initiated by the addition of 30 μl of 2.5 mM ATP, pH 7. Each experiment was terminated by adding nigericin to 0.5 μg/ml. The fluorescence measured after the addition of nigericin was used as the base line from which the relative quenching of the mutant membranes was calculated. Treatments with Ag^+ or Cd^{2+} were carried out in HMK-NO_3 buffer or HMK-Cl buffer, respectively. Inhibition caused by metal treatment was reversed by adding dithiothreitol (DTT) to 2 mM or β-mercaptoethanol (β-MSH) to 4 mM after initiation of quenching with ATP.

Measurement of ATPase Activity—Typically, 10 μg of membrane protein were diluted into 0.9 ml of TM buffer (55.5 mM Tris-SO_4, 0.2 mM $MgSO_4$, pH 7.8). The assay was initiated by the addition of 100 μl of 4 mM ATP supplemented with 0.8 μCi/ml [γ-^{32}P]ATP. After incubation for 6 min at 30 °C, the reaction was stopped by the addition of 800 μl of 11.25% (w/v) trichloroacetic acid and immediately placed on ice for 10 min. Liberated phosphate was extracted from aqueous solution by adding 0.3 ml of 5 M H_2SO_4, 0.6 ml of 6% (w/v) ammonium molybdate, and 3 ml of benzene:isobutanol (1:1) followed by Vortex mixing. After phase separation, 0.5 ml of the organic phase was removed for scintillation counting. For treatments with DCCD, HMK-NO_3 buffer containing membrane protein at 0.5 mg/ml was supplemented with 50 μM DCCD from a 0.1 M ethanolic stock solution and incubated for 20 min at room temperature prior to additional treatment. For silver and cadmium treatments, membrane protein in HMK-NO_3 buffer was incubated with 40 μM $AgNO_3$ or 300 μM $CdCl_2$ for 10 min at room temperature. To measure F_1 dissociation, membranes at 0.5 mg/ml in HMK-NO_3 buffer were incubated at room temperature for 5 min with or without the inclusion of 40 μM $AgNO_3$ or 300 μM $CdCl_2$. Half of this suspension was centrifuged at 541,000 $\times$ *g* for 10 min at room temperature to pellet the membrane vesicles. Membranes were exposed to metal a total of 15 min prior to the ATPase assay. A 10-μg aliquot from the uncentrifuged suspension and an equivalent volume of supernatant from the centrifuged suspension were transferred to TM buffer and assayed as above.

Purification of F_1F_0—The His-tagged F_1F_0 complex was purified as described previously (50, 52). Membrane vesicles from 12 g of plasmid pFV2/strain DK8-transformed cells were suspended at ~20–25 mg/ml in 10 ml of extraction buffer (50 mM Tris-HCl, 100 mM KCl, 250 mM sucrose, 30 mM imidazole, 5 mM $MgCl_2$, 0.1 mM K_2-EDTA, 40 mM 6-aminocaproic acid, 15 mM *p*-aminobenzamidine, 0.2 mM DTT, 0.8% soybean phos-

phatidylcholine (Sigma, Type IV-S), 1% octyl glucoside, 0.5% cholate, 0.5% deoxycholate, 2.5% glycerol, pH 7.5) and incubated at 4 °C with rocking for 30 min. Insoluble material was removed by centrifugation at 541,000 × *g* for 30 min. A 1.25-ml nickel-nitrilotriacetic acid column (His Select, Sigma) was pre-equilibrated with 5 volumes of extraction buffer, and the supernatant fraction of the extract was loaded at a flow rate of 0.18 ml/min. The column was washed with 10 volumes of extraction buffer. Bound protein was eluted with 5 ml of elution buffer (extraction buffer containing 400 mM imidazole) at a flow rate of 0.27 ml/min. Ten 0.5-ml fractions were flash frozen in a dry ice and ethanol slurry and stored at −80 °C. Fractions were screened for F_1F_0 components by SDS-PAGE, and protein concentrations were determined using a modified Lowry method (53).

Reconstitution of F_1F_0 in Liposomes—Liposomes were prepared as described previously (52) with some modifications. Phosphatidylcholine (Sigma, Type IV-S) was suspended at 30 mg/ml in reconstitution buffer (10 mM Tricine-KOH, 2.5 mM $MgSO_4$, 0.1 mM K_2-EDTA, 0.5 mM DTT, pH 8.0) by incubation at 50 °C with periodic mixing with a vortexer. Unilamellar liposomes were produced by sonication (with a Heat Systems Ultrasonics 200R sonicator using a 3-mm probe) on ice twice for 30 s at 20-watt power output with a 1-min interval between sonications. Liposomes were mixed with 10% cholate (1% final concentration) and then with purified F_1F_0 at a protein to lipid ratio of 1:20 and then incubated at 4 °C with rocking for 30 min. This suspension was passed through a centrifuged gel filtration column containing 5 ml of G-25 Sephadex (Sigma) preswollen with reconstitution buffer according to the method of Penefsky (54). At this point, F_1F_0 liposomes were either used immediately for the preparation of F_0 liposomes or frozen in liquid nitrogen for later determination of ATP-driven H^+ pumping activity.

Preparation of K^+-loaded F_0 Liposomes—F_1F_0 liposomes were dialyzed against 1000 volumes of stripping buffer (0.5 mM Tricine, 0.5 mM K_2EDTA, 0.5 mM DTT, pH 8.5) overnight at 4 °C to remove F_1. F_0 liposomes were diluted with stripping buffer lacking DTT and collected by centrifugation at 195,000 × *g* for 20 min and resuspended at 60 mg/ml lipid in HMK-SO_4 buffer (10 mM HEPES-KOH, 2.5 mM $MgSO_4$, 25 mM K_2SO_4, pH 7.5). The suspension was frozen in liquid nitrogen, thawed in cold water, and sonicated in a Bransonic bath sonicator twice for 10 s with an intervening 20-s interval. This procedure was repeated once. K^+-loaded F_0 liposomes were collected by centrifugation at 541,000 × *g* for 10 min and resuspended at 120 mg/ml lipid in HMK-SO_4 buffer. F_0 liposomes were stored at 4 °C and were stable for several days.

Electrical Gradient (Δψ)-driven ACMA Fluorescence Quenching—A 5-μl aliquot of K^+-loaded F_0 liposomes (0.6 mg of lipid) was added to 3.2 ml of stirring HMN-SO_4 buffer (10 mM HEPES-NaOH, 2.5 mM $MgSO_4$, 25 mM Na_2SO_4, pH 7.5) supplemented with 0.3 μg/ml ACMA in a fluorometer cuvette. Quenching of fluorescence was initiated by the addition of valinomycin to 14 ng/ml and terminated by the addition of nigericin to 0.5 μg/ml. For Cd^{2+} treatment, $CdSO_4$ was added to the indicated concentration after the addition of liposomes and ~20 s before the initiation of quenching with valinomycin.

RESULTS

Phenotype and Metal Sensitivity of Cys Substitutions—We report the phenotype and metal sensitivity of function for Cys substitutions in the cytoplasmic loop and the N terminus and C terminus of subunit *c*. This study nearly completes the screening of subunit *c* with 71 of 79 positions tested for function by *in vivo* oxidative phosphorylation, ATP-driven H^+ pumping activity, and its sensitivity to treatment with Ag^+ and Cd^{2+}, and the entirety of this data set is tabulated in Table 1. Most of the new Cys substitution mutants generated in this study grew nearly as well as wild type on both glucose and succinate minimal media (Table 1), indicating a functional oxidative phosphorylation system. Only the R41C substitution abolished growth on succinate, and this substitution was not further characterized. Previous studies determined that Arg-41 is essential for F_1 binding and intolerant of even conservative mutations (24, 25). Inverted membrane vesicles from most of the remaining Cys substitution strains were functional in ATP-driven proton pumping as assayed by ACMA fluorescence quenching (Table 1). For mutant F_1F_0 complexes that were functional in this assay, we tested the effects of 40 μM Ag^+ and 300 μM Cd^{2+} on H^+ pumping as described previously (46, 47). Sensitivity values are tabulated in Table 1. Notably, substitutions at most positions in the loop (residues 33–49) were strongly inhibited by Ag^+ (Table 1). Only the G33C, K34C, and E37C substitutions at the C-terminal end of TMH1 showed minimal inhibition. Substitutions at positions 35 and 42–49 were also sensitive to inhibition by Cd^{2+} (Table 1).

Distinguishing the Mechanisms of Inhibition for the Cytoplasmic Loop Cys Substitutions—Ag^+ and Cd^{2+} react with the thiolate form of Cys, which should predominate in an aqueous *versus* a lipid-exposed environment. In previous studies of Cys substitutions in transmembrane regions, sensitivity to a metal was thought to be indicative of aqueous exposure, and inhibition was thought to reflect direct obstruction of an aqueous proton translocation pathway (41–44, 46, 47). It is possible that substitution of a hydrophobic residue with Cys could introduce novel aqueous accessibility into subunit *c*. However, such a Cys residue would not be expected to be sensitive to metal inhibition of ATP-driven H^+ pumping unless the Cys side chain packed in a position that was proximal to the native H^+ translocation pathway. Cys substitutions outside the membrane should also have access to the bulk aqueous solvent except for those where the side chain is buried in the protein. Ag^+ sensitivity is therefore less likely to reflect blockage of an aqueous proton channel unless the channel continues through a protein domain after exiting the lipid bilayer of the membrane. Alternatively, reaction of Cys in the loop region with a metal may disrupt the binding of F_1 or the coupling of F_1 to F_0 and thus prevent ATP-driven quenching while making membranes proton-permeable. Substitutions in this region have been shown previously to reduce the affinity of F_1 binding to F_0 (22–26), and modification of an ϵH38C mutation at the interface of subunits ϵ and *c* with *N*-ethylmaleimide disrupts F_1 binding (56). To determine whether sensitive residues in the cytoplasmic loop of subunit *c* are directly involved in H^+ transport and/or gating,

TABLE 1
Phenotypic characterization and metal sensitivity of Cys substitution mutants

Substitution	Colony size on succinate[a]	Growth yield on glucose[b]	ATP-driven quenching[c]	Inhibition of H^+ pumping[d]		Ref.
				Ag^+	Cd^{2+}	
	mm	%	%	%		
TMH1						
L9C	2.2	106	74	32	12	This study
Y10C	2.2	104	70	49	13	This study
M11C	2.2	107	76	57	12	This study
A12C	1.7	101	83	32	7	This study
A13C	2.2	107	80	19	8	This study
A14C	2.2	98	82	35	11	This study
V15C	2.0	104	78	8	8	47
M16C	2.2	105	76	5	9	47
M17C	2.0	108	77	1	8	47
G18C	0	62	≤3			47
L19C	2.3	109	76	3	2	47
A20C	2.0	96	75	97	4	47
A21C	2.1	99	78	14	4	47
I22C	2.5	97	76	2	4	47
G23C	0	57	≤3			47
A24C	2.2	98	75	97	13	47
A25C	1.5	80	46	90	5	47
I26C	2.1	97	76	3	8	47
G27C	0.1	56	≤3			47
I28C	2.3	108	72	97	96	47
G29C	0.5	59	≤3			47
I30C	2.0	100	76	0	6	47
L31C	2.0	99	70	16	14	47
G32C	0.1	58	≤3			47
Loop						
G33C	1.9	100	78	36	9	This study
K34C	1.8	100	79	42	12	This study
F35C	1.2	63	47	96	79	This study
L36C	2.2	102	66	94	4	This study
E37C	2.2	97	48	22	9	This study
G38C	2.0	98	63	96	15	This study
A39C	2.0	100	71	91	8	This study
A40C	1.8	100	57	96	14	This study
R41C	0	58				This study
Q42C	1.8	100	81	96	51	This study
P43C	1.8	96	52	96	64	This study
D44C	2.0	102	76	97	91	This study
L45C	1.8	99	73	96	59	This study
I46C	1.5	101	69	97	86	This study
P47C	2.0	104	13[e]			This study
L48C	1.8	102	42	94	66	This study
L49C	2.0	100	61	96	87	This study
R50C[f]	2.0	75	≤3			This study
T51C	2.0	100	≤3			This study
TMH2						
Q52C	2.1	87	61	97	76	46
F53C	2.1	91	64	99	21	46
F54C	2.1	100	6			46
I55C	2.1	95	3			46
V56C	2.2	108	68	97	24	46
M57C	2.0	89	71	97	78	46
G58C	2.1	87	57	99	95	46
L59C	2.1	90	48	84	90	46
V60C	2.2	103	65	99	8	46
D61C	0	65	≤2			46
A62C	1.1	98	78	99	35	46
I63C	2.1	100	74	98	93	46
P64C[g]	2.1	95	69	95	44	46
M65C	2.1	94	66	97	28	46
I66C	2.4	105	73	91	7	46
A67C	2.4	100	67	5	6	46
V68C	2.0	108	82	45	8	46
G69C	2.0	85	71	62	11	46
L70C	2.2	103	79	18	9	46
G71C	2.1	106	77	4	7	46
L72C	2.0	99	69	50	7	This study
Y73C	2.0	79	≤3			This study
V74C	2.2	101	73	87	4	This study
M75C	2.0	100	69	91	3	This study
F76C	2.5	100	29			This study
A77C	2.0	100	27			This study
V78C	2.0	99	78	75	18	This study
A79C	2.0	100	70	33	16	This study

[a] After 72 h of growth at 37 °C. Average colony size of WT is 2.2 mm.
[b] Maximum A_{550} relative to WT on 0.04% glucose. The *unc* deletion strain grows to 60 ± 5% of WT.
[c] Average quenching of wild type is 70 ± 5%.
[d] Extent of reduction in ATP-driven quenching upon metal treatment.
[e] Function was enhanced after treatment with 2 mM DTT suggesting auto-oxidation of this Cys.
[f] Substitutions of Arg-50, Thr-51, and Tyr-73 cause a puzzling phenotype in which mutants grow on succinate but are incapable of ATP-driven H^+ pumping. The phenotype is consistent with Cys substitutions of Phe-54 and Ile-55 described previously (46) and with the *c*D61N/M65D double mutation (55), which supports ATP synthesis but not H^+ pumping.
[g] Constructed with an A20P suppressor mutation.

we sought to distinguish these possible mechanisms of Ag^+ and Cd^{2+} inhibition.

Irreversibility of Metal Inhibition Suggests Disruption of F_1 Binding to F_o—If metal binding to a substituted Cys disrupts F_1 binding to F_0, then removal of the bound metal may not restore function. Conversely, if metal binding simply blocks the H^+ translocation pathway, then function would more likely be restored upon removal of the blocking metal. Binding of Ag^+ or Cd^{2+} to a substituted Cys should be readily reversed by the addition of a metal-chelating agent such as DTT or β-MSH. The thiolates of the reduced forms of these reagents compete with protein Cys residues for the Ag^+ or Cd^{2+} ions causing the inhibition. Extended incubation with DTT reversed Ag^+ inhibition in previous studies of subunit *a* (41), and both DTT and β-MSH have been used in electrophysiological experiments of the cystic fibrosis transmembrane regulator to rapidly reverse silver modifications of Cys substitutions (57). To determine whether treatment with metals disrupts the integrity of the F_1F_0 complex, we attempted to rapidly reverse metal inhibition by treatment with DTT or β-MSH during ATP-driven H^+ pumping.

Inverted membrane vesicles were treated with 40 μM Ag^+ or 300 μM Cd^{2+} and assayed for ATP-driven quenching of ACMA fluorescence. During the quenching assay, DTT or β-MSH was added shortly after the addition of ATP. For most transmembrane Cys substitutions in subunit *c*, addition of DTT or β-MSH immediately reversed inhibition as represented by quenching of ACMA fluorescence for the M57C substitution (Fig. 1*A*). Addition of DTT also reversed inhibition at several Cys substitutions in the loop as represented by the L48C substitution (Fig. 1*B*). The reversal effect is consistent with the removal of a blockage of the H^+ translocation pathway and was seen with most transmembrane substitutions as summarized in Table 2. On the other hand, ≤20% reversal of inhibition was observed for substitutions at positions 40, 42, and 49 in the loop region of subunit *c* (Fig. 1*C* and Table 2), and only partial reversal was observed for substitutions at positions 25, 35, 36, 38, 39, 43, and 52 (Fig. 1*D* and Table 2). Persistence of Ag^+ inhibition after the addition of DTT suggested that metal treatment caused an irreversible alteration of the

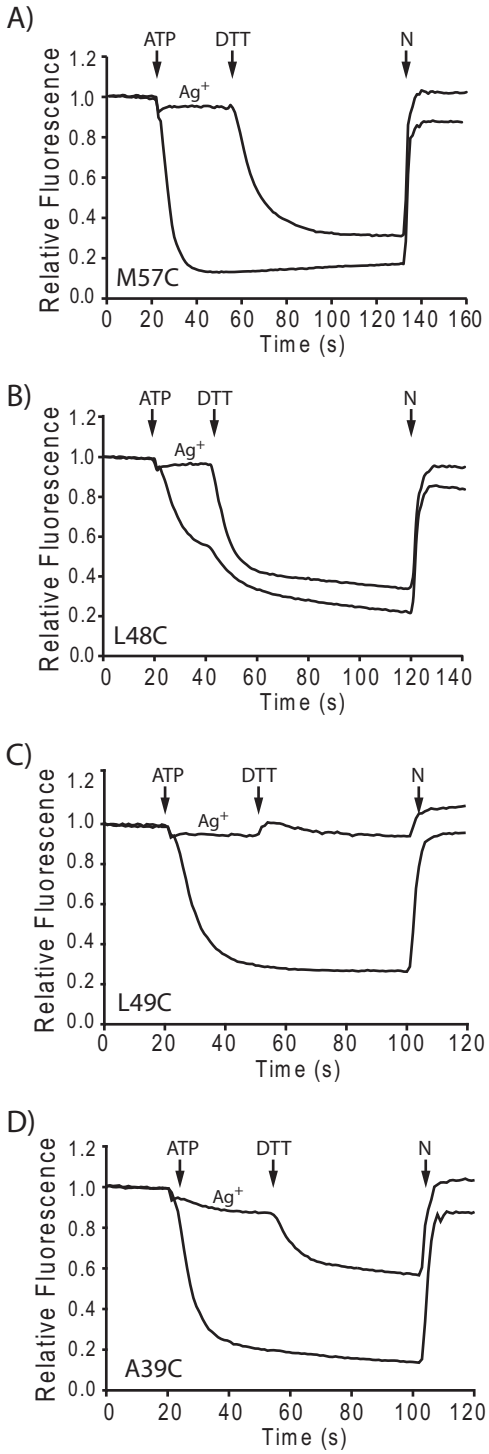

FIGURE 1. **Reversal of Ag^+ inhibition of H^+ pumping by DTT.** Inverted membrane vesicles were incubated at room temperature for 10 min either with or without 40 μM $AgNO_3$ and then assayed for ATP-driven quenching of ACMA fluorescence. In samples treated with Ag^+, 2 mM DTT was added at the time indicated. The times of addition of ATP and nigericin (*N*) are also indicated. *A–D* show fluorescence traces representing reversible inhibition (*A* and *B*), irreversible inhibition (*C*), and partially reversible inhibition (*D*).

Cys-substituted F_1F_0 complex or a slowly reversible alteration where reversal is beyond the time course of the experiment. The lack of reversal is consistent with disruption of the interactions between F_1 to F_0 and possible loss of F_1 from the membrane.

TABLE 2
Reversibility of Ag^+ inhibition of H^+ pumping by DTT

Substitution	Inhibition by Ag^{+a}	Restoration by DTT[b]
	%	%
TM1		
A20C	97	88
A24C	97	78
A25C	90	47
I28C	97	95
Loop		
F35C	96	29
L36C	94	34
G38C	96	24
A39C	91	65
A40C	96	16
Q42C	96	12
P43C	96	70
D44C	97	97
L45C	96	94
I46C	97	100
L48C	94	96
L49C	96	20
TM2		
Q52C	97	69
F53C	99	90
V56C	97	95
M57C	97	96
G58C	99	90
L59C	84	99
V60C	99	83
A62C	99	88
I63C	98	95
P64C[c]	95	75
M65C	97	97
I66C	91	85
V74C	87	94[d]
M75C	91	79[d]

[a] Inhibition of quenching of ACMA fluorescence after the addition of ATP but before the addition of DTT.
[b] Percentage of quenching response restored by DTT relative to the maximum quenching in the absence of Ag^+.
[c] Constructed with an A20P suppressor mutation.
[d] 4 mM β-mercaptoethanol used in place of 2 mM DTT.

Effect of Ag^+ on Dissociation of F_1—To investigate the possibility that the irreversible inhibition of proton pumping by metal binding at some positions in the cytoplasmic loop was caused by disruption of F_1 binding to F_0, we measured the effect of Ag^+ treatment on the ATPase activity of the six substitutions in the *c* loop showing the least reversibility in Ag^+-inhibited ATP-driven H^+ pumping. Inverted membrane vesicles from each substitution were incubated in HMK-NO_3 buffer with 40 μM Ag^+, and then half of this suspension was centrifuged to remove the membranes and any bound ATPase. Equivalent volumes of the suspension before centrifugation and the supernatant fraction after centrifugation were assayed for ATPase activity. No significant release of ATPase activity from wild type membranes was observed even after metal treatment (Fig. 2). For the three substitutions where the Ag^+ inhibition of proton pumping was essentially irreversible (*i.e.* A40C, Q42C, and L49C), only a small fraction of ATPase activity was released from membranes without metal treatment. However, Ag^+ treatment markedly increased the amount of the ATPase activity in the supernatant for each of these substitutions (Fig. 2*A*). Similar results were seen for the G38C substitution. For the two substitutions showing more moderate reversibility, F35C and L36C, approximately a third of the ATPase activity measured in the uncentrifuged membrane suspension was present in the supernatant after centrifugation without metal treatment, sug-

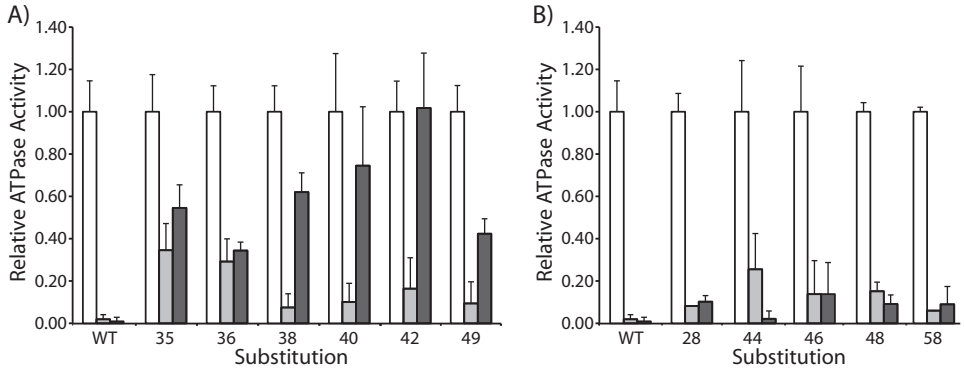

FIGURE 2. **Effect of Ag^+ on the release of F_1 from the membrane.** Inverted membrane vesicles were assayed for ATPase activity. *White bars* indicate the ATPase activity of untreated, uncentrifuged membranes. The substitutions tested showed inhibition of ACMA quenching by Ag^+ that was irreversible (*A*) or reversible (*B*) by DTT treatment. Prior to the assay, membranes in HMK-NO_3 buffer were incubated at room temperature without metal (*light gray bars*) or with 40 μM $AgNO_3$ (*dark gray bars*). After 1 min, half of the membrane suspension was centrifuged to collect the membrane fraction. The *light* and *dark gray bars* indicate the ATPase activity measured in the supernatant fraction expressed as a ratio relative to the total ATPase activity of the untreated membrane suspension. *Error bars* represent the S.D. for each measurement.

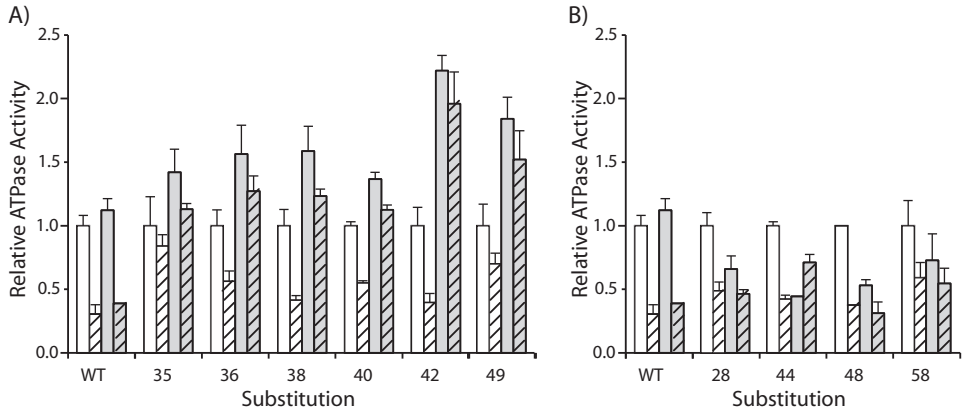

FIGURE 3. **Effects of Ag^+ on total ATPase activity and its sensitivity to DCCD.** Inverted membrane vesicles were assayed for ATPase activity. The substitutions tested showed inhibition of ACMA quenching by Ag^+ that was irreversible (*A*) or reversible (*B*) following treatment with DTT. Prior to the assay, membranes were incubated for 20 min at room temperature in HMK-NO_3 buffer with no additions (*solid bars*) or 50 μM DCCD (*hatched bars*). These incubations were followed by treatment with no metal (*white bars*) or 40 μM $AgNO_3$ (*gray bars*). Activity is expressed as a ratio relative to the activity of untreated membranes. *Error bars* represent the S.D. for each measurement.

gesting that the Cys substitutions themselves cause a degree of disruption of F_1 binding to F_0 (Fig. 2*A*). Treatment with Ag^+ did not significantly further increase the ATPase activity released from the membranes of these mutants. For substitutions classified as fully reversible (*i.e.* I28C, D44C, I46C, L48C, and G58C), only a small amount of ATPase activity was released without metal treatment, and treatment with Ag^+ did not significantly increase the activity released to the supernatant (Fig. 2*B*).

Effects of Ag^+ and Cd^{2+} on Total ATPase Activity and Its Sensitivity to DCCD—Disruption of the functional coupling of F_1 and F_0 during Ag^+ or Cd^{2+} treatment with or without release of F_1 from the membrane surface should reduce the sensitivity of ATPase activity to DCCD, an inhibitor that specifically modifies Asp-61 of subunit *c* and blocks H^+ translocation with a consequential inhibition of F_1-ATPase activity. To test the effects of metals (both Ag^+ and Cd^{2+}) on DCCD sensitivity, which is a measure of the coupling of F_1 to F_0, inverted membrane vesicles were incubated with or without 50 μM DCCD for 30 min at room temperature, and for the final 10 min of incubation, samples were treated with or without 40 μM Ag^+ (or 300 μM Cd^{2+}). The ATPase activity of these membrane suspensions was then assayed. For wild type membranes, Ag^+ slightly stimulated activity (Fig. 3). DCCD inhibited wild type ATPase activity by 70 $\pm$ 5%, and inhibition was not significantly affected by metal treatment. The ATPase activities of L36C, G38C, A40C, Q42C, and L49C membrane suspensions were greatly stimulated by treatment with Ag^+, and metal treatment strikingly reduced the DCCD sensitivity of the reaction, most strikingly for the A40C substitution (Fig. 3*A*). We observed similar effects after Cd^{2+} treatment of Q42C and L49C (data not shown). The enhancement of ATPase activity can be attributed to the release of F_1-ATPase from the membrane (as shown in Fig. 2) with removal of the drag resistance by the F_0 rotary motor on the F_1 rotary motor. The loss of DCCD sensitivity on metal treatment of the L36C, G38C, A40C, Q42C, and L49C substitutions supports the conclusion that F_1 is uncoupled from F_0. In contrast, the ATPase activity of Cys substitutions thought to be involved in H^+ translocation (*i.e.* mutants where metal inhibition was reversed by DTT) was inhibited by Ag^+ in a manner similar to the inhibition observed after treatment with DCCD (Fig. 3*B*). In the case of transmembrane residues I28C and G58C and loop residue L48C, DCCD inhibition of ATPase activity was not reversed by Ag^+ (Fig. 3*B*).

Effect of Cd^{2+} on H^+ Transport through F_o—To support the hypothesis that Ag^+ and Cd^{2+} block H^+ translocation in the Cys substitutions where inhibition was reversed by DTT, we directly measured the effects of metal treatment on H^+ transport by Cys-substituted F_0. We reconstituted wild type and mutant F_0 into liposomes and measured the quenching of ACMA fluorescence driven by a $\Delta\psi$. As described under "Experimental Procedures," His-tagged F_1F_0 was purified by detergent extraction and affinity chromatography and then reconstituted into unilamellar phosphatidylcholine liposomes. F_1 was removed under conditions of high pH and low ionic strength, and the resultant F_0 liposomes were loaded with K^+. To measure H^+ influx through F_0, we diluted K^+-loaded F_0 liposomes into a K^+-free buffer containing ACMA and added valinomycin to generate a $\Delta\psi$ in response to the K^+ diffusion potential, which then drove H^+ import into the liposomes through F_0. Ag^+ interfered with the valinomycin-driven quenching assay likely because of its affinity for valinomycin (58), so we only examined Cd^{2+}-sensitive mutants here. Wild type F_0 and several mutant F_0 complexes containing Cys substitutions in subunit *c* were purified and functionally reconstituted; however, complexes containing mutations F35C, D44C, L49C, M57C, G58C, and I63C were not successfully reconstituted. To determine whether Cd^{2+} when bound to a substituted Cys blocks H^+ permeability, we supplemented the $\Delta\psi$-driven quenching assay with various concentrations of $CdSO_4$. Wild type F_0 was minimally sensitive with <15% inhibition being seen at 300 μM Cd^{2+} (Fig. 4). Cd^{2+} markedly reduced the quenching response of F_0 liposomes with I28C or L59C transmembrane substitutions and markedly inhibited the quenching response of the I46C and L48C loop substitutions (Fig. 4). The Cd^{2+} inhibition of this quenching response, which directly measures passive H^+ translocation through F_0, strongly suggests that Cd^{2+} also inhibits ATP-driven H^+ pumping in these four mutants by directly blocking H^+ transport through F_0. Relative to that seen in wild type, Cd^{2+} treatment resulted in somewhat greater inhibition of the quenching response with Q42C, L45C, or Q52C F_0 liposomes (Fig. 4), which suggested that the structural changes causing uncoupling upon metal treatment may also result in minor effects on H^+ movement through the loop region at the surface of F_0. The relatively minor inhibition observed for these substitutions is consistent with the conclusion that uncoupling is the primary mechanism of metal inhibition at these positions.

Flexibility of the Cytoplasmic Loop—The length of the cytoplasmic loop of subunit *c* (*i.e.* the number of residues between the conserved G*X*G*X*G*X*G motif in TMH1 and the Asp-61 or equivalent residue in TMH2 is invariant among the *c* subunits of eubacteria and eukaryotes (Fig. 5*A*)) and an NMR study of the loop from *E. coli* subunit *c* suggested that it forms a rigid structure (59). We tested the structural flexibility of the region of the cytoplasmic loop implicated in H^+ translocation by inserting or deleting 1–3 residues near Ile-46 (Fig. 5*B*). This region of the loop was chosen for alteration due to its low sequence conservation. Residues were genetically inserted or deleted by oligonucleotide-directed mutagenesis as described under "Experimental Procedures." We then assayed the insertion or deletion mutants for ATP-driven H^+ pumping to determine whether the alterations disrupted activity. To our surprise, inverted membrane vesicles from mutants in which Ile-46 was deleted or Ala was inserted after Leu-45 were functional in ATP-driven proton pumping as assayed by ACMA fluorescence quenching (Fig. 5*C*). Mutants in which Ile-46 and Leu-48 were both deleted or Ala-Gly-Ala was inserted after Leu-45 were not functional in this assay (Fig. 5*C*).

Metal-mediated Cross-linking at Some Cys Positions—A third effect of Ag^+ may contribute to inhibition at several positions. Ag^+ is multicoordinate and has been shown to simultaneously bind multiple thiolates (60). A Cys substituted into subunit *c* would be present in every subunit making up the decameric ring so that any substituted Cys would be in close proximity to the Cys in subunits on either side. Single Cys substitutions at the C-terminal end of *c*TMH2 have been shown to form dimers in the presence of Cu^{2+}-phenanthroline (15), and other cross-linking experiments indicate that *c*TMH2 is capable of significant mobility (61). To test the possibility that inhibition of H^+ pumping could be caused by metal-mediated cross-linking, we have created genetically fused subunit *c* dimers that contain a single substituted Cys in only one copy of the two fused subunits. A *c*-ring assembled from these dimers would not position Cys in adjacent subunits, so formation of a metal-mediated cross-link would be unlikely. Inverted membrane vesicles isolated from these fusion mutants are competent in ATP-driven proton pumping as assayed by quenching of ACMA fluorescence (Table 3). When assayed for Ag^+ sensitivity, most dimer substitutions retained the sensitivity observed in the Cys-substituted *c* monomer, suggesting that cross-linking is not the source of inhibition for these sensitive substitutions. Marked reductions in Ag^+ sensitivity occurred for several substitutions on the periplasmic half of subunit *c*, including *c*′A20C, *c*′V60C, *c*′M75C, and *c*′V78C where the *c*′ substitution is placed in only the C-terminal subunit of the *c*-*c*′ dimer. A reduction in sensitivity to Ag^+ resulting from increased spacing between Cys suggests that metal-mediated cross-linking may contribute significantly to inhibition at these positions. This conclusion for *c*′M75C and *c*′V78C is supported by Cu^{2+}-mediated cross-linking of these residues, suggesting increased flexibility in the C terminus (15). On the other hand, a more likely explanation for the *c*(wild type)-*c*′A20C and *c*(wild type)-*c*′V60C dimers may be a reduced disruption of structure in rigidly packed regions of the *c*-ring, especially for the V60C substitution, which lies on the buried side of TMH2 proximal to TMH1.

DISCUSSION

Previous studies demonstrated that Ag^+ and Cd^{2+} ions and presumably H_2O can access Cys substitutions in the transmembrane regions of subunit *c* and defined an aqueous pathway by which protons can travel from the proton-binding Asp-61 in the middle of the membrane to the cytoplasmic surface (46, 47). In the current study, we surveyed the Ag^+ and Cd^{2+} sensitivity of Cys substitutions in the polar loop and at the N- and C-terminal ends of subunit *c* and identified several Ag^+-sensitive regions lying outside of the membrane bilayer with distinctly different properties. Two distinct regions were identified in the cytoplasmic loop. In the first region including residues between

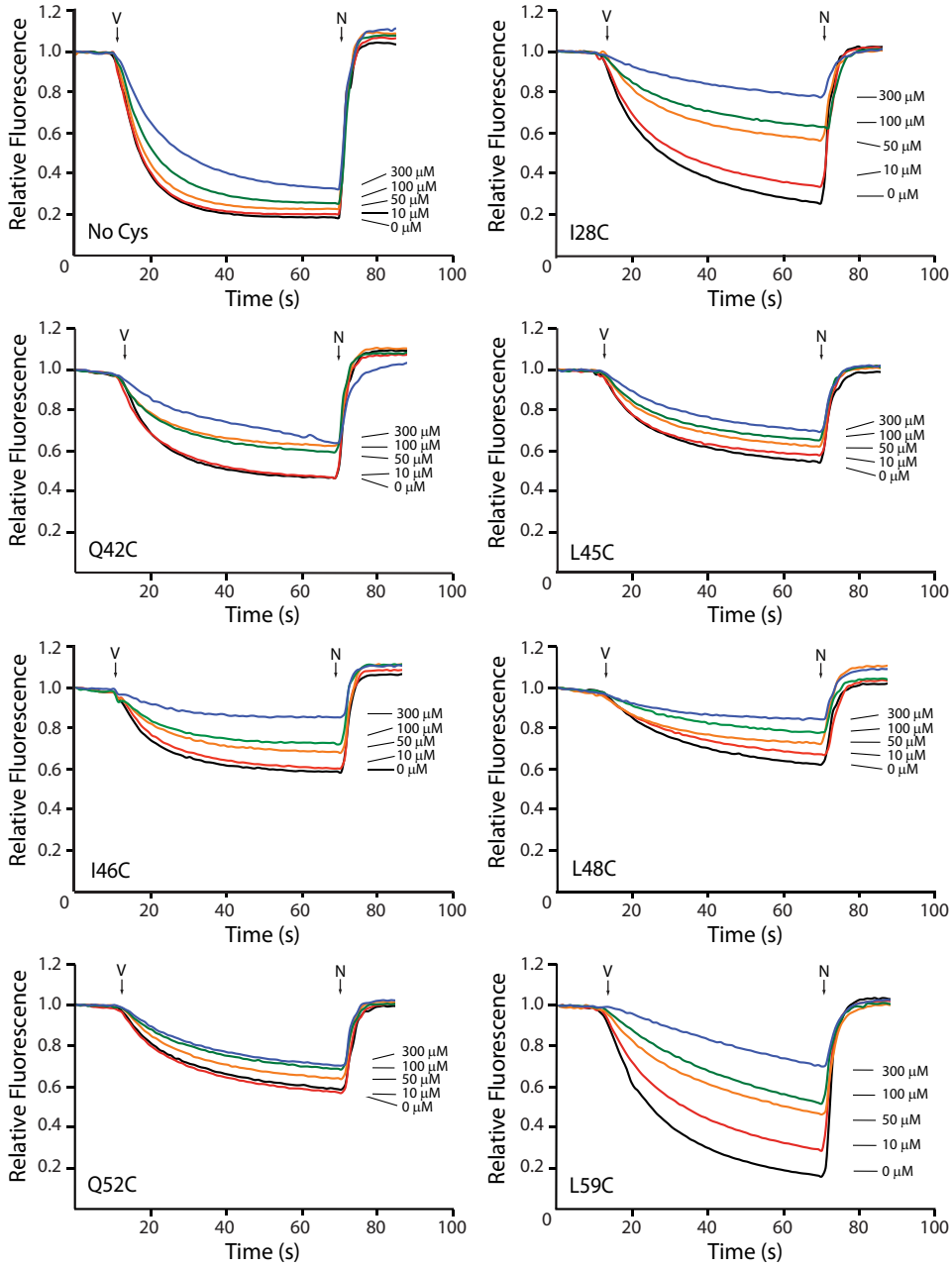

FIGURE 4. **Effect of Cd^{2+} on the H^+ permeability of reconstituted F_0.** The H^+ permeability of K^+-loaded F_0 liposomes was assayed by $\Delta\psi$-driven quenching of ACMA fluorescence as described under "Experimental Procedures." After base-line fluorescence was established with 0.6 mg of F_0 liposomes, quenching was initiated by the addition of valinomycin (*arrow V*). $CdSO_4$ was included at the indicated concentration. Quenching was stopped by the addition of nigericin (*arrow N*).

positions 35 and 43 on the N-terminal side and 49 and 52 on the C-terminal side of the loop (Fig. 6), substitutions became uncoupled upon treatment with Ag^+ or Cd^{2+}, suggesting that metal treatment of Cys substitutions in this region disrupts F_1 binding to the *c*-ring. In a second region of the loop including residues 44–48 (Fig. 6), metals inhibited ATP-coupled H^+ transport without uncoupling F_1 from F_0, and Cd^{2+} was shown to block passive F_0-mediated H^+ transport, suggesting that this was the mechanism of inhibition. Finally, in the C-terminal region at positions 74–78, inhibition appeared to be the result of Ag^+-mediated cross-linking between Cys in adjacent *c* subunits in the ring. This hypothesis is plausible given that Ag^+ is bicoordinate (60) and that Cys substitutions at positions 74, 75, and 78 form high yield dimers in the presence of Cu^{2+}-phenanthroline, suggesting structural flexibility in this region (15).

Most of the metal-inhibited Cys substitutions in the loop, including positions 35, 36, 38–43, 49, and 52, show defects in the binding or coupling of F_1 to F_0 as initially evidenced by the irreversibility of inhibitory effects of Ag^+ by subsequent addition of DTT. At the positions studied in greater detail, metal treatment resulted in increased F_1 release from the membrane with a resultant increase in ATPase activity, reduced DCCD sensitivity, and Ag^+ inhibition of H^+ pumping that was unaffected or only partially reversed by treatment with DTT (Figs. 2 and 3). These effects are consistent with previous mutagenesis results supporting the role of this region in F_1 binding. Arg-41,

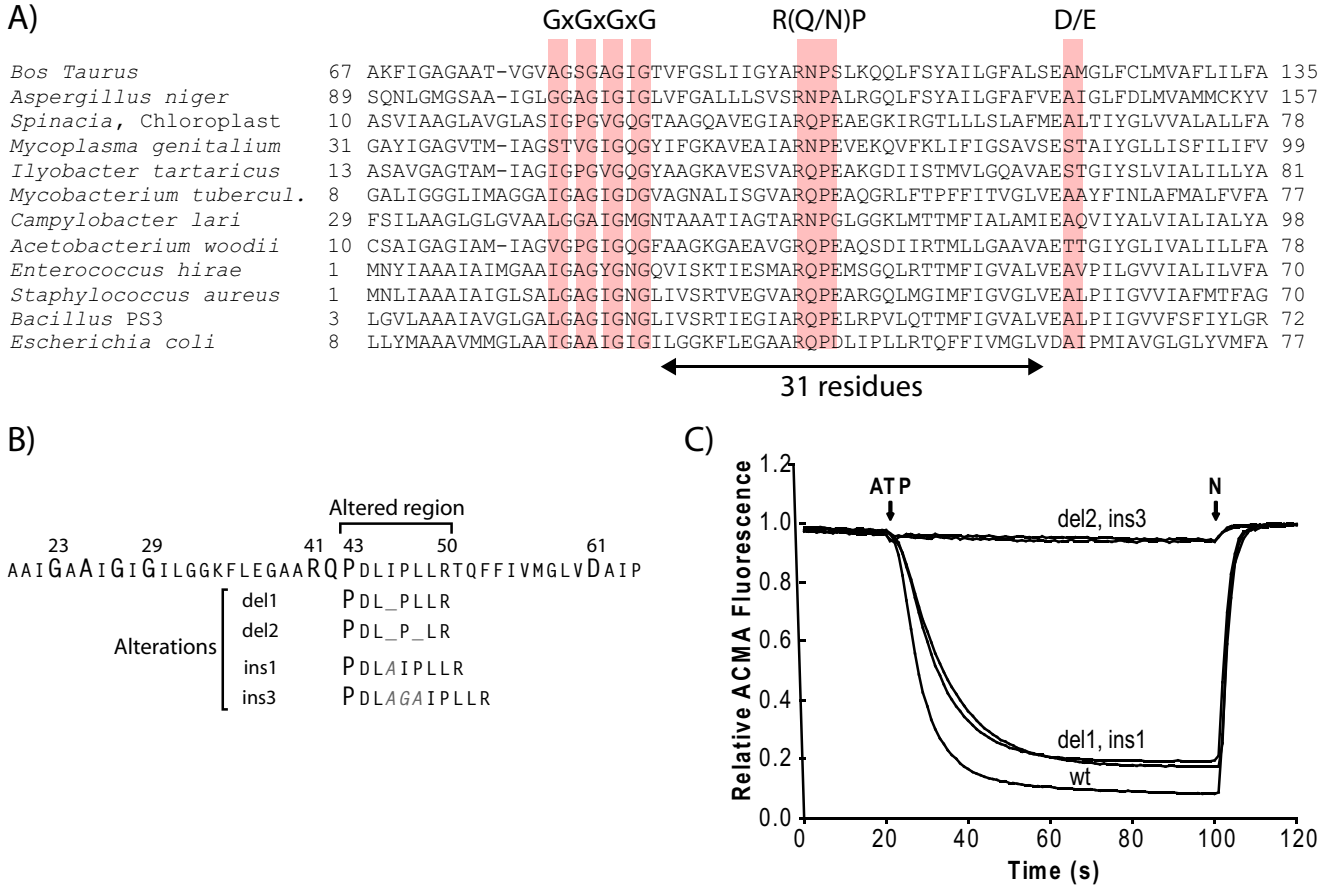

FIGURE 5. **Function of mutants with an altered subunit *c* loop.** *A*, alignment of subunit *c* sequences from various bacterial and eukaryotic species indicates a distance of 31 residues between the helix packing motif (G*X*G*X*G*X*G) and the proton binding motif (*D/E*). *B*, a portion of the amino acid sequence of *E. coli* subunit *c* is shown with conserved motifs marked in *bold*. Deletions (*del*) or insertions (*ins*) of amino acids (marked in *gray italics*) were made in the subunit *c* loop downstream of the conserved RQP motif. *C*, inverted membrane vesicles containing F_1F_0 with an altered subunit *c* loop were assayed for ATP-driven quenching of ACMA fluorescence in HMK-CI buffer. Fluorescence traces are labeled to correspond to the alterations described in *A*. *N*, nigericin.

TABLE 3
Sensitivity of fused c dimers to Ag^+

Substitution	ATP-driven quenching by c_2	Inhibition by Ag^+	
		c^{Cys}	$c_2^{WT/Cys}$
	%	%	
A12C	69	32	29
A20C	73	97[a]	44
A24C	59	97[a]	95
I28C	42	97[a]	94
L36C	78	94	70
A40C	47	96	90
L48C	43	94	95
L49C	72	96	95
Q52C	18	95[b]	81
F53C	71	95[b]	97
V56C	55	96[b]	90
G58C	39	97[b]	95
V60C	72	97[b]	25
I63C	51	96[b]	94
M75C	74	91	29
V78C	65	75	42

[a] Reported in Ref. 47.
[b] Reported in Ref. 46.

Gln-42, and Pro-43 form a conserved motif, and in general, mutations in this region are characterized by reduced binding affinity of the *c*-ring with F_1, increased dissociation of F_1, reduced DCCD sensitivity, and a defect in ATP-driven H^+ pumping, all of which are indicators of defective coupling of F_1 and F_0 (21–27). The deleterious effect of a Q42E mutation in this motif can be suppressed by a second, compensating mutation at Glu-31 in subunit ϵ (26). Furthermore, disulfide cross-linking experiments indicate that Cys at positions 40, 42, 43, and 44 can be cross-linked to subunits γ and ϵ in F_1 (28, 29, 56).

A recent structure of the F_1c complex from yeast mitochondria revealed the *c*-$\gamma\epsilon$ interface at high resolution and supports the electrostatic interaction of this region of the loop with the F_1 stalk (62). Ag^+ or Cd^{2+} modification of a Cys at this position might easily alter the chemical environment required for F_1 binding. Despite its role as a binding site for the γ and ϵ subunits of F_1, the loop is remarkably tolerant of substitution, even at the latter two positions in the highly conserved RQP motif. This tolerance is consistent with the results of a random mutagenesis study where mutants with substitutions at every position in the loop except for Arg-41 still supported growth on succinate (63). In a striking example of loop plasticity, we observed that ATP-driven H^+ pumping activity is not significantly affected by the insertion of an Ala after Leu-45 or the deletion of Ile-46 even though the length of the loop is invariant across bacterial and eukaryotic *c* subunits (Fig. 5*A*).

We have also identified a region of the loop in which binding of metals to Cys block ATP-coupled H^+ transport in a manner that was totally reversed by DTT as was the case for most transmembrane substitutions. This region includes positions 44–48

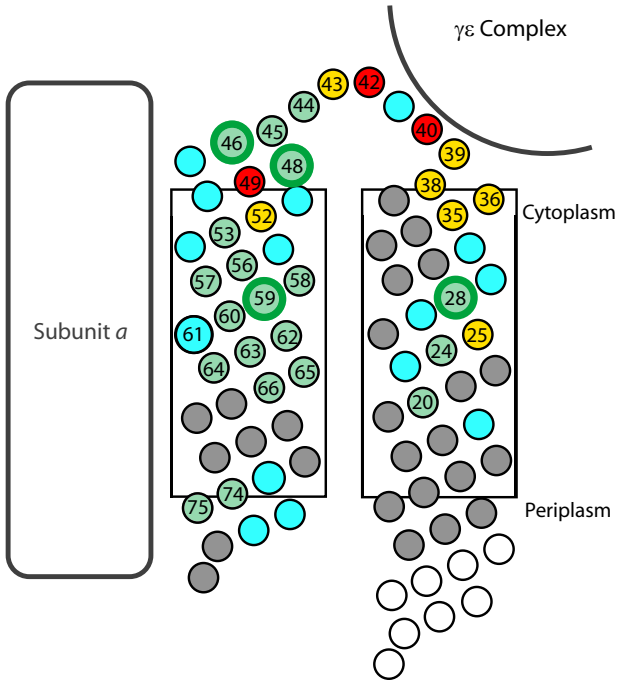

FIGURE 6. **Two distinct regions of metal sensitivity in the polar loop of subunit *c*.** Residues in subunit *c* are shown as *circles*. Cys substitutions of the numbered residues were Ag^+-sensitive in this and previous studies (46, 47). *Circles* are colored to represent the reversibility of Ag^+ inhibition upon treatment with DTT: *green* indicates essentially full reversibility (≥70%), *yellow* indicates partial reversibility (>20–70%), and *red* indicates little or no reversibility (≤20%). *Enlarged green circles* indicate residues where Cd^{2+} blocked passive H^+ translocation. *Gray circles* represent residues that were not sensitive to Ag^+. Positions where a Cys substitution abolishes function are colored *cyan*. Positions colored *white* were not tested. The approximate proximity of other F_1F_0 subunit domains is indicated.

and is continuous with the aqueous accessible cytoplasmic end of TMH2. Two of the loop substitutions also show passive F_0-mediated proton transport activity that was inhibited by Cd^{2+} in a manner akin to the inhibition seen with representative transmembrane substitutions where metals are thought to inhibit function by directly blocking proton transport through F_0. These two Cys substitutions, *i.e.* I46C and L48C, show no indication of dissociation of F_1 from F_0 on treatment with Ag^+ or Cd^{2+}. Two other Cys substitutions in this region, D44C and L45C, also show complete reversal of inhibition by DTT and no evidence of uncoupling F_1 from F_0. In addition, metal treatment was shown to inhibit ATPase activity for several representative substitutions both in this region of the loop and in TMH substitutions in contrast to the metal-dependent stimulation of ATPase activity in mutants that became uncoupled (Figs. 2 and 3). Although the effects of Ag^+ on the H^+ permeability of F_0 could not be tested, the common chemistry shared by Ag^+ and Cd^{2+} in sulfur chelation as well as the identical effects caused by both metals for many substitutions in the other assays reported here (*i.e.* inhibition of ATP-driven H^+ pumping, reversibility of inhibition by DTT, and inhibition of ATPase activity) suggests that Ag^+ also blocks H^+ translocation in these regions (64). These results support our previous interpretations (41–44, 46, 47) that the sensitivity of substitutions in transmembrane regions to Ag^+ and Cd^{2+} is due to blockage of the H^+ translocation pathway and that accessibility to the metals is provided by an aqueous channel that functions in F_0-mediated H^+ transport.

The occurrence of metal sensitivity in the residue 44–48 region of the loop that is likely to be caused by steric or electrostatic blockage of H^+ transport suggests that the H^+ translocation pathway does not end at the surface of the lipid bilayer but rather continues through a protein domain into the cytoplasm. Although the structure of the *E. coli c*-ring has not been determined, several crystal structures of H^+-translocating *c*-rings indicate that residues 46 and 48 lie on the end of TMH2 and project toward each other at the interface of two *c* subunits (17, 19, 20, 62, 65). Furthermore, residue 44 projects into the cytoplasm from the loop. The arrangement of the side chains of residues 46 and 48 suggests that the H^+ translocation pathway may run at the interface of two *c* subunits packing against subunit *a* in this region. Recently, Moore *et al.* (45) reported on the Ag^+ sensitivity of two Cys substitutions in the 1-2 loop and substitutions in the 194–199 region of the 3-4 loop of subunit *a*. Cross-linking experiments showed that the residues in the 1-2 loop, including M93C, lie in close proximity to the highly Ag^+-sensitive L195C substitution. The authors concluded that these Ag^+-sensitive regions pack into a single cytoplasmic domain that is somehow involved in the H^+ translocation pathway, perhaps as part of a gating mechanism. Residues 194–199 in the 3-4 loop lie at the cytoplasmic end of TMH4 just outside of the membrane, and earlier cross-linking studies (35) indicate that an extensive face of the cytoplasmic side of *a*TMH4 packs against *c*TMH2 in the membrane. These observations suggest that the Ag^+-sensitive residues in the 3-4 loop of subunit *a* lie in close proximity to the portion of the cytoplasmic loop of subunit *c* proposed in this study to be involved in H^+ translocation. Given the expected proximity of *a*M93C to the region of the subunit *c* loop implicated here in H^+ translocation, interaction between each of these Ag^+-sensitive domains is a reasonable expectation. The exit channel at the *a*TMH4 and *c*TMH2 interface from the middle of the membrane to the cytoplasm may then be gated by interacting cytoplasmic domains of the polar loop of subunit *c* and the cytoplasmic loops of subunit *a*.

Acknowledgments—We thank Rachael Patterson, Hun Sun Chung, and Andrew Larkin for assistance with some of these experiments. Professor Wayne Frasch of Arizona State University generously provided the pFV2 plasmid. We also thank Drs. Robert Nakamoto and Christoph von Ballmoos for helpful suggestions on the preparation of F_O liposomes.

REFERENCES

1. Yoshida, M., Muneyuki, E., and Hisabori, T. (2001) ATP synthase—a marvellous rotary engine of the cell. *Nat. Rev. Mol. Cell Biol.* **2,** 669–677
2. Nakamoto, R. K., Baylis Scanlon, J. A., and Al-Shawi, M. K. (2008) The rotary mechanism of the ATP synthase. *Arch. Biochem. Biophys.* **476,** 43–50
3. von Ballmoos, C., Wiedenmann, A., and Dimroth, P. (2009) Essentials for ATP synthesis by F_1F_0 ATP synthases. *Annu. Rev. Biochem.* **78,** 649–672
4. Foster, D. L., and Fillingame, R. H. (1982) Stoichiometry of subunits in the H^+-ATPase complex of *Escherichia coli*. *J. Biol. Chem.* **257,** 2009–2015
5. Jiang, W., Hermolin, J., and Fillingame, R. H. (2001) The preferred stoichiometry of *c* subunits in the rotary motor sector of *Escherichia coli* ATP synthase is 10. *Proc. Natl. Acad. Sci. U.S.A.* **98,** 4966–4971

6. Mitome, N., Suzuki, T., Hayashi, S., and Yoshida, M. (2004) Thermophilic ATP synthase has a decamer *c*-ring: indication of noninteger 10:3 H^+/ATP ratio and permissive elastic coupling. *Proc. Natl. Acad. Sci. U.S.A.* **101,** 12159–12164
7. Meier, T., Polzer, P., Diederichs, K., Welte, W., and Dimroth, P. (2005) Structure of the rotor ring of F-type Na^+-ATPase from *Ilyobacter tartaricus*. *Science* **308,** 659–662
8. Pogoryelov, D., Yu, J., Meier, T., Vonck, J., Dimroth, P., and Muller, D. J. (2005) The c15 ring of the *Spirulina platensis* F-ATP synthase: F_1/F_0 symmetry mismatch is not obligatory. *EMBO Rep.* **6,** 1040–1044
9. Watt, I. N., Montgomery, M. G., Runswick, M. J., Leslie, A. G., and Walker, J. E. (2010) Bioenergetic cost of making an adenosine triphosphate molecule in animal mitochondria. *Proc. Natl. Acad. Sci. U.S.A.* **107,** 16823–16827
10. Stock, D., Leslie, A. G., and Walker, J. E. (1999) Molecular architecture of the rotary motor in ATP synthase. *Science* **286,** 1700–1705
11. Boyer, P. (1989) A perspective of the binding change mechanism for ATP synthesis. *FASEB J.* **3,** 2164–2178
12. Abrahams, J. P., Leslie, A. G., Lutter, R., and Walker, J. E. (1994) Structure at 2.8 Å resolution of F_1-ATPase from bovine heart mitochondria. *Nature* **370,** 621–628
13. Noji, H., Yasuda, R., Yoshida, M., and Kinosita, K. (1997) Direct observation of the rotation of F_1-ATPase. *Nature* **386,** 299–302
14. Weber, J., and Senior, A. E. (2003) ATP synthesis driven by proton transport in F_1F_0-ATP synthase. *FEBS Lett.* **545,** 61–70
15. Jones, P. C., Jiang, W., and Fillingame, R. H. (1998) Arrangement of the multicopy H^+-translocating subunit *c* in the membrane sector of the *Escherichia coli* F_1F_0 ATP synthase. *J. Biol. Chem.* **273,** 17178–17185
16. Dmitriev, O. Y., Jones, P. C., and Fillingame, R. H. (1999) Structure of the subunit *c* oligomer in the F_1F_o ATP synthase: model derived from solution structure of the monomer and cross-linking in the native enzyme. *Proc. Natl. Acad. Sci. U.S.A.* **96,** 7785–7790
17. Vollmar, M., Schlieper, D., Winn, M., Büchner, C., and Groth, G. (2009) Structure of the c14 rotor ring of the proton translocating chloroplast ATP synthase. *J. Biol. Chem.* **284,** 18228–18235
18. Krah, A., Pogoryelov, D., Langer, J. D., Bond, P. J., Meier, T., and Faraldo-Gómez, J. D. (2010) Structural and energetic basis for H^+ versus Na^+ binding selectivity in ATP synthase F_o rotors. *Biochim. Biophys. Acta* **1797,** 763–772
19. Pogoryelov, D., Yildiz, O., Faraldo-Gómez, J. D., and Meier, T. (2009) High-resolution structure of the rotor ring of a proton-dependent ATP synthase. *Nat. Struct. Mol. Biol.* **16,** 1068–1073
20. Preiss, L., Yildiz, O., Hicks, D. B., Krulwich, T. A., and Meier, T. (2010) A new type of proton coordination in an F_1F_0-ATP synthase rotor ring. *PLoS Biol.* **8,** e1000443
21. Mosher, M. E., White, L. K., Hermolin, J., and Fillingame, R. H. (1985) H^+-ATPase of *Escherichia coli*. An *uncE* mutation impairing coupling between F_1 and F_0 but not F_0-mediated H^+ translocation. *J. Biol. Chem.* **260,** 4807–4814
22. Miller, M. J., Fraga, D., Paule, C. R., and Fillingame, R. H. (1989) Mutations in the conserved proline 43 residue of the *uncE* protein (subunit *c*) of *Escherichia coli* F_1F_0-ATPase alter the coupling of F_1 to F_0. *J. Biol. Chem.* **264,** 305–311
23. Fraga, D., and Fillingame, R. H. (1989) Conserved polar loop region of *Escherichia coli* subunit *c* of the F_1F_0 H^+-ATPase. Glutamine 42 is not absolutely essential, but substitutions alter binding and coupling of F_1 to F_0. *J. Biol. Chem.* **264,** 6797–6803
24. Hatch, L., Fimmel, A. L., and Gibson, F. (1993) The role of arginine in the conserved polar loop of the *c*-subunit of the *Escherichia coli* H^+-ATPase. *Biochim. Biophys. Acta* **1141,** 183–189
25. Fraga, D., Hermolin, J., Oldenburg, M., Miller, M. J., and Fillingame, R. H. (1994) Arginine 41 of subunit *c* of the *Escherichia coli* H^+-ATP synthase is essential in binding and coupling of F_1 to F_0. *J. Biol. Chem.* **269,** 7532–7537
26. Zhang, Y., Oldenburg, M., and Fillingame, R. H. (1994) Suppressor mutations in F_1 subunit ϵ recouple ATP-driven H^+ translocation in uncoupled Q42E subunit *c* mutant of *Escherichia coli* F_1F_0 ATP synthase. *J. Biol. Chem.* **269,** 10221–10224
27. Zhang, Y., and Fillingame, R. H. (1995) Subunits coupling H^+ transport and ATP synthesis in the *Escherichia coli* ATP synthase. *J. Biol. Chem.* **270,** 24609–24614
28. Watts, S. D., Zhang, Y., Fillingame, R. H., and Capaldi, R. A (1995) The γ subunit in the *Escherichia coli* ATP synthase complex (ECF_1F_0) extends through the stalk and contacts the *c* subunits of the F_0 part. *FEBS Lett.* **368,** 235–238
29. Hermolin, J., Dmitriev, O. Y., Zhang, Y., and Fillingame, R. H. (1999) Defining the domain of binding of F_1 subunit ϵ with the polar loop of F_0 subunit *c* in the *Escherichia coli* ATP synthase. *J. Biol. Chem.* **274,** 17011–17016
30. Pogoryelov, D., Nikolaev, Y., Schlattner, U., Pervushin, K., Dimroth, P., and Meier, T. (2008) Probing the rotor subunit interface of the ATP synthase from *Ilyobacter tartaricus*. *FEBS J.* **275,** 4850–4862
31. Valiyaveetil, F. I., and Fillingame, R. H. (1998) Transmembrane topography of subunit *a* in the *Escherichia coli* F_1F_0 ATP synthase. *J. Biol. Chem.* **273,** 16241–16247
32. Long, J. C., Wang, S., and Vik, S. B. (1998) Membrane topology of subunit *a* of the F_1F_0 ATP synthase as determined by labeling of unique cysteine residues. *J. Biol. Chem.* **273,** 16235–16240
33. Wada, T., Long, J. C., Zhang, D., and Vik, S. B. (1999) A novel labeling approach supports the five-transmembrane model of subunit *a* of the *Escherichia coli* ATP synthase. *J. Biol. Chem.* **274,** 17353–17357
34. Schwem, B. E., and Fillingame, R. H. (2006) Cross-linking between helices within subunit *a* of *Escherichia coli* ATP synthase defines the transmembrane packing of a four-helix bundle. *J. Biol. Chem.* **281,** 37861–37867
35. Jiang, W., and Fillingame, R. H. (1998) Interacting helical faces of subunits *a* and *c* in the F_1F_0 ATP synthase of *Eschericia coli* defined by disulfide cross-linking. *Proc. Natl. Acad. Sci. U.S.A.* **95,** 6607–6612
36. Moore, K. J., and Fillingame, R. H. (2008) Structural interactions between transmembrane helices 4 and 5 of subunit *a* and the subunit *c* ring of *Escherichia coli* ATP synthase. *J. Biol. Chem.* **283,** 31726–31735
37. Fillingame, R. H., Angevine, C. M., and Dmitriev, O. Y. (2003) Mechanics of coupling proton movements to *c*-ring rotation in ATP synthase. *FEBS Lett.* **555,** 29–34
38. Karlin, A., and Akabas, M. H. (1998) Substituted-cysteine accessibility method. *Methods Enzymol.* **293,** 123–145
39. Kaback, H. R., Dunten, R., Frillingos, S., Venkatesan, P., Kwaw, I., Zhang, W., and Ermolova, N. (2007) Site-directed alkylation and the alternating access model for LacY. *Proc. Natl. Acad. Sci. U.S.A.* **104,** 491–494
40. Lü, Q., and Miller, C. (1995) Silver as a probe of pore-forming residues in a potassium channel. *Science* **268,** 304–307
41. Angevine, C. M., and Fillingame, R. H. (2003) Aqueous access channels in subunit *a* of rotary ATP synthase. *J. Biol. Chem.* **278,** 6066–6074
42. Angevine, C. M., Herold, K. A., and Fillingame, R. H. (2003) Aqueous access pathways in subunit *a* of rotary ATP synthase extend to both sides of the membrane. *Proc. Natl. Acad. Sci. U.S.A.* **100,** 13179–13183
43. Angevine, C. M., Herold, K. A., Vincent, O. D., and Fillingame, R. H. (2007) Aqueous access pathways in ATP synthase subunit *a*. Reactivity of cysteine substituted into transmembrane helices 1, 3, and 5. *J. Biol. Chem.* **282,** 9001–9007
44. Dong, H., and Fillingame, R. H. (2010) Chemical reactivities of cysteine substitutions in subunit *a* of ATP synthase define residues gating H^+ transport from each side of the membrane. *J. Biol. Chem.* **285,** 39811–39818
45. Moore, K. J., Angevine, C. M., Vincent, O. D., Schwem, B. E., and Fillingame, R. H. (2008) The cytoplasmic loops of subunit *a* of *Escherichia coli* ATP synthase may participate in the proton translocating mechanism. *J. Biol. Chem.* **283,** 13044–13052
46. Steed, P. R., and Fillingame, R. H. (2008) Subunit *a* facilitates aqueous access to a membrane-embedded region of subunit *c* in *Escherichia coli* F_1F_0 ATP synthase. *J. Biol. Chem.* **283,** 12365–12372
47. Steed, P. R., and Fillingame, R. H. (2009) Aqueous accessibility to the transmembrane regions of subunit *c* of the *Escherichia coli* F_1F_0 ATP synthase. *J. Biol. Chem.* **284,** 23243–23250
48. Barik, S. (1996) Site-directed mutagenesis *in vitro* by megaprimer PCR. *Methods Mol. Biol.* **57,** 203–215
49. Jones, P. C., Hermolin, J., and Fillingame, R. H. (2000) Mutations in single hairpin units of genetically fused subunit *c* provide support for a rotary

catalytic mechanism in F_0F_1 ATP synthase. *J. Biol. Chem.* **275,** 11355–11360
50. Ishmukhametov, R. R., Galkin, M. A., and Vik, S. B. (2005) Ultrafast purification and reconstitution of His-tagged cysteine-less *Escherichia coli* F_1F_0 ATP synthase. *Biochim. Biophys. Acta* **1706,** 110–116
51. Klionsky, D. J., Brusilow, W. S., and Simoni, R. D. (1984) *In vivo* evidence for the role of the ϵ subunit as an inhibitor of the proton-translocating ATPase of *Escherichia coli*. *J. Bacteriol.* **160,** 1055–1060
52. Wiedenmann, A., Dimroth, P., and von Ballmoos, C. (2008) $\Delta\psi$ and ΔpH are equivalent driving forces for proton transport through isolated F_0 complexes of ATP synthases. *Biochim. Biophys. Acta* **1777,** 1301–1310
53. Fillingame, R. H. (1976) Purification of the carbodiimide-reactive protein component of the ATP energy-transducing system of *Escherichia coli*. *J. Biol. Chem.* **251,** 6630–6637
54. Penefsky, H. S. (1979) A centrifuged-column procedure for the measurement of ligand binding by beef heart F_1. *Methods Enzymol.* **56,** 527–530
55. Langemeyer, L., and Engelbrecht, S. (2007) Essential arginine in subunit *a* and aspartate in subunit c of F_oF_1 ATP synthase: effect of repositioning within helix 4 of subunit *a* and helix 2 of subunit *c*. *Biochim. Biophys. Acta* **1767,** 998–1005
56. Aggeler, R., Weinreich, F., and Capaldi, R. A. (1995) Arrangement of the ϵ subunit in the *Escherichia coli* ATP synthase from the reactivity of cysteine residues introduced at different positions in this subunit. *Biochim. Biophys. Acta* **1230,** 62–68
57. Alexander, C., Ivetac, A., Liu, X., Norimatsu, Y., Serrano, J. R., Landstrom, A., Sansom, M., and Dawson, D. C. (2009) Cystic fibrosis transmembrane conductance regulator: using differential reactivity toward channel-permeant and channel-impermeant thiol-reactive probes to test a molecular model for the pore. *Biochemistry* **48,** 10078–10088
58. Reed, P. W. (1979) Ionophores. *Methods Enzymol.* **55,** 435–454
59. Dmitriev, O. Y., and Fillingame, R. H. (2007) The rigid connecting loop stabilizes hairpin folding of the two helices of the ATP synthase subunit *c*. *Protein Sci.* **16,** 2118–2122
60. Bell, R., and Kramer, J. (1999) Structural chemistry and geochemistry of silver-sulfur compounds: critical review. *Environ. Toxicol. Chem.* **18,** 9–22
61. Vincent, O. D., Schwem, B. E., Steed, P. R., Jiang, W., and Fillingame, R. H. (2007) Fluidity of structure and swiveling of helices in the subunit *c* ring of *Escherichia coli* ATP synthase as revealed by cysteine-cysteine cross-linking. *J. Biol. Chem.* **282,** 33788–33794
62. Dautant, A., Velours, J., and Giraud, M.-F. (2010) Crystal structure of the Mg·ADP-inhibited state of the yeast F_1c_{10}-ATP synthase. *J. Biol. Chem.* **285,** 29502–29510
63. Fraga, D., and Fillingame, R. H. (1991) Essential residues in the polar loop region of subunit *c* of *Escherichia coli* F_1F_0 ATP synthase defined by random oligonucleotide-primed mutagenesis. *J. Bacteriol.* **173,** 2639–2643
64. Steed, P. R. (2010) *Proton Transport at the Interface of Subunit c and the Rotor Ring of Escherichia coli ATP Synthase.* Ph.D. thesis, University of Wisconsin-Madison
65. Saroussi, S., Schushan, M., Ben-Tal, N., Junge, W., and Nelson, N. (2012) Structure and flexibility of the C-ring in the electromotor of rotary F_0F_1-ATPase of pea chloroplasts. *PLoS One* **7,** e43045